

# N-acetylcysteine modulation of mitochondrial respiration and blood brain barrier permeability is time dependent and cell type specific

## Abstract

One common symptom of most neurodegenerative diseases related to aging is the presence of blood-brain barrier disruption and mitochondrial dysfunction. N-acetylcysteine (NAC) is an FDA approved drug commonly utilized for a variety of neuropsychiatric and neurodegenerative diseases; however, while studies have shown that NAC can improve mitochondrial function in mouse models of some of these diseases, the mechanism(s) of action have yet to be fully defined. Our previous studies have shown that NAC treatment can alter blood-brain barrier (BBB) permeability in mice via changes in reactive oxygen species (ROS). To further examine the effects of NAC on both cell-specificity and the mitochondrial respiration of brain vascular endothelial cells and astrocytes that make up the blood-brain barrier, we utilized brain microvascular endothelial and cerebrum astrocytic cells and an in vitro mouse BBB model. We show that NAC caused time- and dose-dependent changes in BBB permeability that were correlated to significant changes in tight and gap junction proteins, change in endothelial nNOS, and downregulation of mitochondrial complex proteins in endothelial cells. Extracellular flux analysis revealed a significant reduction in endothelial cell mitochondrial maximal respiration after 48hrs. In contrast, astrocyte respiration showed no change after 48hours but was significantly increased after 24hours of NAC treatment corresponding to the decreased permeability noted at this time. These changes paralleled alterations in NOS in endothelial cells but not astrocytes. We conclude that murine astrocytes and endothelial cells respond to NAC treatment in a cell-specific fashion, altering their perspective metabolic profiles and ultimately the tight and gap junctions that determine the permeability of the BBB. Given the current theory that mitochondrial dysfunction and BBB leakiness are predisposing, possibly causative symptoms, for most neurodegenerative diseases associated with aging, our findings suggest that NAC's cell-specific effects upon both metabolism and BBB permeability may be concurrent mechanisms by which this drug is effective.

**Keywords:** astrocyte, blood-brain barrier, endothelium, metabolism, mitochondria

Volume 3 Issue 6 - 2018

**Salim S El Amouri, Christopher A Waker, Luping Huang, Cameron L Smith, Debra A Mayes**

Department of Neuroscience, Cell Biology and Physiology, Wright State University, USA

**Correspondence:** Debra A Mayes, Department of Neuroscience, Cell Biology & Physiology, Wright State University Boonshoft School of Medicine, College of Science and Math, 3640 Colonel Glenn Highway, 451 Neuroscience Engineering Collaboration Building, Dayton, OH 45435, USA, Tel 513-680-2258, Email [debra.mayas@wright.edu](mailto:debra.mayas@wright.edu)

**Received:** October 31, 2018 | **Published:** November 16, 2018

**Abbreviations:** BBB, blood brain barrier; TJs, tight junctions; GJ, gap junction; ROS, reactive oxygen species; TEER, transendothelial electrical resistance; OCR, oxygen consumption rate; NAC, n-acetylcysteine

## Introduction

The blood brain barrier (BBB) is an active boundary between circulating blood and brain interstitial fluids which functions to regulate the brain's microenvironment. The barrier restricts transport of cells or toxins into the CNS and regulates the transport of nutrients and metabolites in and out of the brain. The BBB is formed from endothelial cells, adjacent astrocytic end feet, and pericytes of brain vasculature. These cells are connected through a complex set of proteins called tight junctions (TJs) which form a physical barrier forcing most molecules to traffic through tightly controlled, selective transcellular routes—forming a transport barrier. The TJs between endothelial cells are structural proteins responsible for BBB function.<sup>1,2</sup> TJs are composed of a combination of trans-membrane and cytoplasmic proteins linked to an action-based cytoskeleton, which allows these junctions to form a tight seal.<sup>3</sup> Occludin and the claudins are endothelial TJ proteins that are essential for brain barrier functions.<sup>4,5</sup> It has been shown that claudin-5 is a critical regulator of brain endothelial cell permeability.<sup>6</sup> Although some evidence

indicates that occludin is not essential in the formation of a TJ, its decreased expression has been associated with BBB dysfunction in a number of diseases.<sup>7-10</sup>

In addition to endothelial TJs, there is a synergistic relationship between brain endothelial cells and astrocytes. Perivascular astrocytic endfeet surround brain endothelial cells but are separated by a basal lamina. These astrocytic endfeet associate with one another and other cells through gap junction (GJ) bridges made up of connexin hexamers. GJs regulate the intracellular and extracellular concentration and transport of a wide range of small molecules including Ca<sup>2+</sup> and ATP. This is particularly interesting because Ca<sup>2+</sup> and ATP are known to regulate BBB tightness either directly or indirectly.<sup>11-13</sup> The importance of astrocytes and GJs in BBB function has been indicated in a recent study showing that disruption of BBB integrity can occur by a GJ-dependent mechanism;<sup>13</sup> however, how astrocytic GJs modulate BBB permeability is not known.

It has been accepted that increased blood-brain barrier (BBB) permeability is one pathological symptom found in most if not all neurodegenerative diseases associated with aging;<sup>14</sup> however, researchers have yet to determine whether the increase in BBB permeability is an initiating factor or consequence of disease symptomology. Mitochondrial dysfunction is also a co-founding symptom found in most neurodegenerative diseases, and

studies correlating these phenomena have led to the hypothesis that mitochondrial dysfunction may cause increases in BBB permeability.<sup>15,16</sup> Several drug therapies that are thought to act upon the mitochondria have been shown to improve BBB leakiness, providing some credence to this theory.

Our previous work has shown that both the transcription and function of TJ and GJ proteins are regulated by reactive oxygen species (ROS)—indicating that redox status plays an important role in BBB tightness.<sup>17</sup> Moreover, multiple studies and trials have examined the use of antioxidants to regulate BBB permeability. One commonly used antioxidant is N-acetyl- cysteine (NAC). NAC is an FDA approved drug and nutritional supplement used as a mucolytic agent and in the management of acetaminophen overdose in children. It has been successfully tried as a treatment for a number of psychiatric disorders including schizophrenia, bipolar disorder, autism, obsessive-compulsive disorder, depression and addiction.<sup>18</sup> NAC has also proven to be beneficial in multiple animal and clinical trials for a variety of neurodegenerative diseases including Alzheimer's and Parkinson's disease, ALS, stroke, encephalitis, multiple sclerosis.<sup>19</sup> These beneficial effects have been hypothesized to result from NAC's reduction of cellular ROS, which have been correlate to changes in BBB permeability; however, theories have yet to be proven. Previously, we have shown that BBB permeability is dependent upon ROS/NOS levels, with barrier permeability and resulting brain pathology increasing when ROS was too high or low. For example, treatment with the broad-spectrum antioxidant NAC was capable of loosening BBB permeability in normal wild type mice, but tightened the BBB and improved the hyperactive behavior in transgenic animal models in which ROS levels were high. Because NAC's mechanism of action has been theorized to work through mitochondrial regulation, we hypothesized that the NAC-induced BBB permeability changes noted in this study were ROS/NOS-dependent. NAC's mechanism(s) of action on brain vascular endothelial cells and astrocytes that make up the blood-brain barrier (BBB) have not been elucidated. Because metabolic respiration, and it's cellular biproduct reactive oxygen species (ROS), has been linked to the regulation of BBB tight and gap junctions, the current study aimed to determine whether NAC-induced BBB permeability changes do indeed correlate with both functional metabolic alterations and tight and gap junction changes.

In the present study, we investigated the effect of NAC on the modulation of BBB permeability in an *in vitro* wild-type BBB murine model and characterized the role of mitochondrial metabolism regulation (the largest ROS producer) in this process in order to begin to understand the possible cell-specific role(s) of mitochondrial respiration in NAC-induced BBB permeability/regulation. We correlated mitochondrial respiration and BBB permeability modulation data to NAC-induced changes in the tight junctions claudin<sup>5</sup> and occludin, the gap junctions connexin-43 and connexin-37, ROS and NOS expression.

These studies are important for two reasons. First, the ability to use NAC, an already FDA-approved drug, to open or close the BBB in both normal and pathological animals suggests that this drug could be utilized prior to drug treatment to allow non-permeable drugs to enter the brain. However, in order to utilize this new treatment modality, the mechanism(s) of action would need to be further studied. The current study begins to address this issue. The cell- specificity of NAC's function upon the brain vascular endothelial cells and astrocytes is novel and highlights the differences in metabolic function at the BBB.

## Material and methods

### Cell culture

In order to be able to correlate previous mouse model work with an *in-vitro* blood brain barrier model, astrocytes and endothelial cells from a mouse line were required. Immortalized mouse brain microvascular endothelial cells, b End3, and the mouse cerebellum astrocytic cell line (C8-D1A) were obtained from American Type Culture Collection (CRL-299; CRL-2541, respectively, Manassas, VA). Both cell lines were cultured in Dulbecco's modified Eagle's medium (DMEM) (Sigma, St. Louis, MO) with 10% fetal bovine serum (FBS) (Hyclone, Logan, UT), 4mM L-glutamine (Sigma, St. Louis, MO) and 1% penicillin–streptomycin (PS) (Sigma, St. Louis, MO). Cells (passage 1–15) were maintained in a humidified cell culture incubator at 37°C and with 5% CO<sub>2</sub>/95% air. Cells for each experiment were passage-matched.

### Murine In vitro BBB model

Trans-well inserts (0.4-μm pore size, 12-well; Corning) were coated with a combination of collagen I+ IV (40:60, collagen I: collagen IV, v/v) on the luminal side, and 0.01% Cultrex Poly- L-Lysine (R&D Systems) on the abluminal side of the insert. Astrocytes were seeded onto the abluminal side of the filter at a density of 2.0×10<sup>4</sup> cells per filter and grown for 2 days. The bEnd3 cells were seeded onto the luminal side of the filter at a density of 1.0×10<sup>5</sup> cells per insert and grown for 6 days. Blank inserts without cells were used as controls for transendothelial electrical resistance (TEER) and permeability measurements.

### Measurement of transendothelial electrical resistance (TEER)

The TEER of the *in vitro* BBB models grown on Transwell inserts were recorded using an Endohm chamber connected to an EVOM resistance meter (World Precision Inst. Inc). TEER of each well was calculated after subtracting the TEER of the blank Transwell inserts and reported as Ωcm<sup>2</sup>. TEER of 100 Ωcm<sup>2</sup> was used as a means to validate the permeability assays (described below).

### Permeability measurements

Permeability of b End.3 and astrocyte monolayers cultured on Transwell inserts was assayed using FITC-labelled dextran-2000 (i.e. 2,000Da, Fisher Scientific). After 24 or 48hrs of NAC treatment, 50μl of FITC-dextran-2000 (1mg/ml) dissolved in a complete culture media (DMEM) was added to the endothelial side of each insert. After 20 minutes of incubation at 37°C, and 5% CO<sub>2</sub> incubation, 200μl of media from the basal chamber (600μl) was used to measure FITC-dextran fluorescent intensity. All readings were measured as duplicates at constant 'gain' settings using Synergy H1 Multi-Mode Reader (BioTek) at excitation: 494nm, and emission: 521nm. The values obtained were plotted on graph pad and checked for significance. Changes in fluorescent intensity in regards to backgrounds (intensities obtained from Transwells without cells or with cells but non-treated with NAC) were calculated and expressed as percentage increase or decrease (mean±SEM) in fluorescence intensity

### NAC treatment

Unless otherwise indicated, bEnd3 endothelial cells or C8-D1A astrocytes were treated with 0.0125% (w/v) in DMEM media. For transwell inserts, 150μl was applied to the apical side of the brain

endothelium, and 500µl was added to basal chamber. Cell cultures in 96, 12 and 6 well plates were incubated with DMEM media containing NAC of 150µl, 1ml, and 2ml, respectively.

### Cell viability and proliferation assays

Control and NAC treated cells were seeded at a density of  $2.0 \times 10^4$  cells per well in 96 well plates. After 24 and 48hrs of NAC treatment, control and NAC treated cells were stained with trypan blue dye to check for viability and total cell counts were performed. Stained cells were counted and viability was calculated as the total cells per well.

### Measurement of reactive oxygen species (ROS)

Cells, bEnd3 endothelial cells and C8-D1A astrocytes, were seeded in 96 well plates ( $2.0 \times 10^4$  cells per well). After 24hrs, cells were treated with 0.0125% NAC or 70µM of L-NAME (a selective inhibitor for NOS isoforms) in DMEM media.<sup>20</sup> Cells were then allowed to grow for 24hrs in a humidified cell culture incubator at 37°C/5% CO<sub>2</sub>. After incubation in DMEM growth media, cells were treated with 10µM CM-H2DCFDA in PBS, for 30 min at 37°C in the dark. After removing excess probe, the cells were suspended in PBS and incubated for 1hr at 37°C in the dark. Total cellular ROS measurements from each well were then measured with a fluorometer (Synergy H1 Multi-Mode Reader; excitation: 495, emission: 527nm). Control wells containing PBS and 10µM CM-H2DCFDA were used to correct for background. ROS activity from treated cells was expressed as % change from control non-treated cells.<sup>21</sup>

### Antibodies

**The primary antibodies used included:** Complex I subunit NDUFB8 (Invitrogen, 1:1000 dilution), Complex IV subunit IV (Invitrogen, 1:1000 dilution), Complex V (ATP Synthase) subunit alpha (Invitrogen, 1:1000 dilution), Claudin-5 (Invitrogen, 1:1000 dilution), Occludin (Invitrogen, 1:1000 dilution), Connexin 43 (Invitrogen, 1:1000 dilution), Connexin 37 (Invitrogen, 1:1000 dilution), NOS1, NOS2, and NOS3 (Cell signaling technology, 1:1000). GAPDH (Enzo life sciences, 1:5000). Cytochrome C (EMD Millipore, 1:2000). The secondary antibodies used included: HRP-conjugated anti-rabbit or anti-mouse antibodies (Santa cruz biotechnology, 1:1000).

### Western blot assays

BCA protein assay was performed to determine the total protein concentration of each sample using a Pierce BCA Assay Protein Kit. Western blots were performed as described previously.<sup>17</sup> Quantification of proteins was performed using Image Studio Lite Western blot analysis software, and band intensities were normalized as a ratio to corresponding load control values. A two-way ANOVA with Turkey Post-hoc testing was performed to determine statistical significance using Sigma Plot v14.0. technical replicates=3-6 well/experiment repeated 3 times.

### Mitochondrial protein isolation

This mitochondrial isolation procedure is a modified version of the mitochondrial isolation protocol provided by Cold Springs Harbor Laboratory Press (Cold Spring Harb Protoc; doi:10.1101/pdb.prot080002).<sup>22</sup> Samples were incubated in RBS hypobuffer containing 1% phosphatase inhibitor cocktail 2, 1% phosphatase inhibitor cocktail 3, 1% phenylmethylsulfonyl fluoride, and 4% complete EDTA-free protease inhibitor cocktail for five minutes before being homogenized for ten minutes using a micro tube homogenizer. After homogenization,  $2.5 \times$  MS homogenization buffer

was added to each sample. The samples were mixed by inversion five times, transferred to a 1.5mL microcentrifuge tube, centrifuged for five minutes ( $1,300g$  at 4°C), and the supernatant was transferred to a new 1.5mL microcentrifuge tube. This process was performed three times, transferring to a new 1.5mL microcentrifuge tube each time. After the third round, supernatant was centrifuged for fifteen minutes ( $12,000g$  at 4°C). The remaining supernatant after this final centrifugation was transferred to a new 1.5mL microcentrifuge tube. The pellet from the final centrifugation was resuspended with 100µL of  $1 \times$  MS homogenization buffer (1% phosphatase inhibitor cocktail 2, 1% phosphatase inhibitor cocktail 3, 1% phenylmethylsulfonyl fluoride, and 4% complete EDTA-free protease inhibitor cocktail). The three pellets, the final supernatant, and the resuspended sample were all frozen and stored at -80°C.

### Extracellular flux analysis

Oxygen consumption rate (OCR) and extracellular acidification rate (ECAR) were measured using a Seahorse XF24 analyzer with the XF Cell Mito Stress Test Kit and XF Glycolysis Stress Test Kit (Agilent Technologies, Santa Clara, CA USA), according to the manufacturer's instructions. In brief, cells were grown to approximately 70–80% confluence in complete DMEM, trypsinized, and seeded in 100-µL volume at 60,000 cells per well in an XF24 cell culture microplate. Cells were incubated at 37°C/5% CO<sub>2</sub> for 3 hours. Culture medium was changed, and the plates were incubated at 37°C/0% CO<sub>2</sub> for 1 hour before the assay. OCR was calculated after sequential additions of oligomycin A, FCCP, antimycin A, and rotenone using an XF Cell Mito Stress Test Kit. The ECAR was calculated after sequential additions of glucose, oligomycin, and 2-DG using an XF Glycolysis Stress Test Kit. All measurements were recorded at set 3:3:3 interval time points. Materials were obtained from Agilent Technologies.

### Statistical analysis

All comparisons were performed between control vehicle-treated and NAC-treated astrocytes or endothelial cell lines (technical replicates, 3-5/experiment), and experiments were repeated 3-4 times using cells from the same passage number. We therefore assume the data fall within a sufficient normal distribution of variance. Technical replicates were averaged, the mean representing one experiment and counted as a single n—providing an n=3-4 for statistical analysis. Extracellular Flux experiments consisted of 10 technical replicates/experiment with 3-5 repeat experiments, because the plastic dishes, only available through Agilent Biosciences, have proven to increase result variability (experimental results from an array optimization studies on the plates, data not shown). Results were expressed as arithmetic mean and standard deviation as specified in the figure legends. Statistical analysis was performed using two-tailed Student's t tests for single comparisons and ANOVA with Turkey posthoc for multiple data sets 3 or larger. 95% confidence intervals were considered to be statistically significant. No randomization or blinding was performed.

## Results

### Dose-dependent NAC-induced BBB permeability changes

To evaluate BBB permeability *in vitro*, we utilized murine brain endothelial, bEnd3, and astrocytic, C8-D1A, cell lines to represent the brain vasculature and surrounding astrocytes in the BBB. Several studies have shown that bEnd3 cells are a suitable immortalized mouse brain endothelial cell line that can be used as a model for BBB 20-20.



Unlike primary cultures, b End 3 don't lose BBB characteristics over repeated passages. They form functional barriers and respond similar to primary cultures when challenged.<sup>20</sup> Similarly, the C8-D1A astrocyte cell line has been well characterized to mimics fibrous astrocytes present in the brain.<sup>22–25</sup> This cell line is usually used as an alternative to primary astrocytes. Therefore, both cell lines, bEnd3 and C8-D1A, have been commonly used to model BBB for permeability studies *in vitro*. The transwell model depicted in Figure 1A is a common *in vitro* BBB model system because it allows endothelial cells and astrocytes to touch one another through the transwell mesh, enabling the formation of a tight barrier. Using this model, permeability can be measured via alteration of trans-endothelial electrical resistance (TEER) or FICT-dextran movement, both of which were measured. Previous studies using this system have provided useful insights about BBB in ischemia, CNS disease progression, and drug delivery studies.

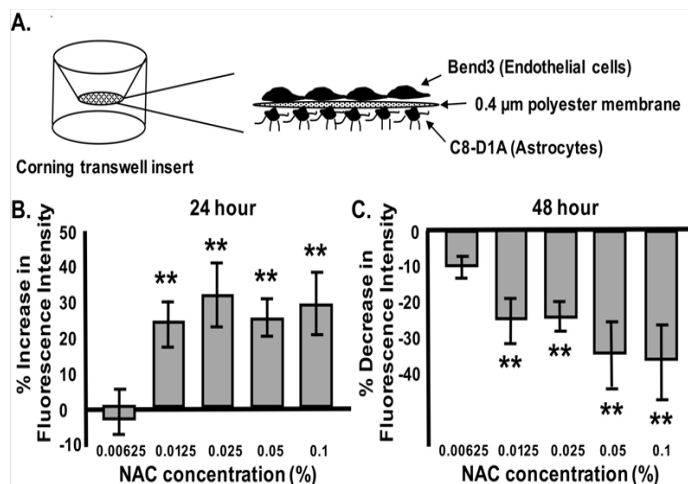


**Figure 1** Dose-dependent NAC-induced BBB permeability changes are time-dependent.

Graphical depiction of *in vitro* Transwell BBB model with b End 3 endothelial cells and C8-D1A astrocyte monocultures grown on each side of a Boyden chamber membrane (A). Percentage FITC-dextran fluorescent intensity after 24hrs (B) or 48hrs (C) of NAC treatment at increasing concentrations (0.00625, 0.125, 0.025, 0.05 and 0.1%). n=3-6/experiment repeated 3 times. ANOVA with Tukey posthoc analysis. Values represent mean  $\pm$ SD. \* $P < 0.05$ , \*\* $P < 0.02$ .

Our previous studies have shown that NAC can change BBB permeability *in vivo* utilizing Evans Blue dye permeability, Electron Microscopic vascular analysis, and biochemical analysis of BBB tight and gap junction proteins<sup>17</sup>. Data from this previous study indicated that there is a critical window in which ROS regulation causes BBB leakiness, suggesting the concept that NAC dose may be a vital element in this regulation. In the current studies, we examined the role of NAC dose on BBB permeability *in vitro*. We utilized different concentrations of NAC (0.0625, 0.0125, 0.025, 0.05, and 0.1%) for 24 and 48hrs. BBB permeability was shown to be concentration dependent after treatment for 24hrs (Figure 1B) or 48hrs (Figure 1C). At 0.0125%, NAC treatment for 24hrs significantly increased the BBB permeability up to 24.5 $\pm$ 8.9% when compared to control. Higher NAC concentrations (0.025%, 0.5% and 0.1%) also induced significant permeability increases (32.1 $\pm$ 13.0, 25.4 $\pm$ 6.1, and 28.9 $\pm$ 8.9), respectively.<sup>26–30</sup>

Surprisingly, after 48hrs of continuous NAC treatment, NAC (0.0125%) caused a decrease in BBB permeability (14.2 $\pm$ 8.4%) when compared to non-treated controls. Higher concentrations of NAC (0.025%, 0.5% and 0.1%) after 48hrs of treatment also significantly decreased permeability (16.33 $\pm$ 7.3, 23.3 $\pm$ 17.2, and 24.8 $\pm$ 17), respectively. NAC treatment studies throughout the rest of this

manuscript were completed using 0.0125% NAC, as it was the lowest dose with significant effects.

## NAC-induced TJ and GJ changes in endothelial cells and astrocytes

NAC has multiple varied mechanisms of action in a cell. For instance, NAC can affect several signaling pathways involved in apoptosis, angiogenesis, cell growth and arrest, redox-regulated gene expression, and the inflammatory response.<sup>27</sup> To better understand possible molecular actions of NAC upon BBB permeability, we examined whether NAC (0.0125%) had an effect on tight and gap junction proteins known to be highly expressed in the BBB. While treatment of monoculture endothelial cells with 0.0125% NAC for 24hrs did not result in a significant decline in the tight junction claudin-5 (Figure 2B), immunohistochemistry revealed that claudin-5 proteins were no longer clustered along the plasma membrane of the endothelial cells and appeared more diffusely dispersed at this time point. There was a significant decreased in occludin protein expression (21.0 $\pm$ 2.6%) when compared to occluding expression in vehicle-treated cells (Figure 2B). The down-regulation occludin and the dispersal of claudin<sup>5</sup> correspond to the increased permeability noted after 24 hours of NAC exposure (Figure 1B).

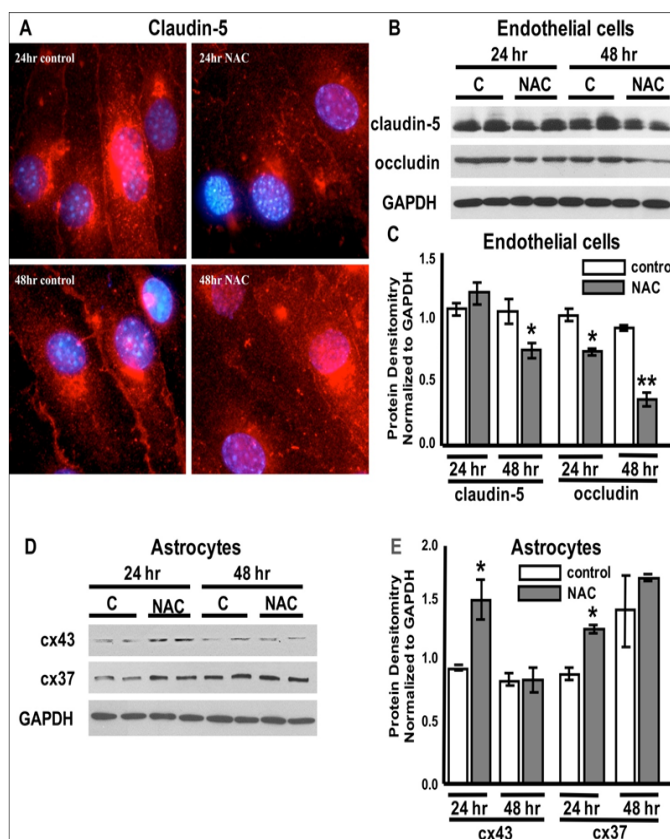


**Figure 2** NAC-induced tight junction (TJ) and gap junction (GJ) changes in endothelial cells and astrocytes.

Representative claudin-5 (red) tight junction immunohistochemistry in b End 3 endothelial cells in vehicle-treated controls and cells exposed to 24 or 48 hours of NAC (0.0125%). Cells are double-labeled with DAPI (blue). Representative Western blots of cell lysates from bEnd3 cells (B) and astrocytes (D) from control, vehicle-treated cells labeled "C" and cells post NAC treatment for 24hrs or 48hrs labeled "NAC". TJ proteins (Claudin-5 and Occludin), GJ proteins (Connexin-43 (cx43) and Connexin-47 (cx47)), and GAPDH. Quantification of protein expression (C, E, respectively). n = 3-6/experiment repeated 3 times. ANOVA with Tukey posthoc analysis. Values represent mean  $\pm$ SD. \* $P < 0.02$ , \*\* $P < 0.01$ .

48hrs post NAC treatment, expression levels for both claudin and occludin were significantly decreased ( $25.0 \pm 2.6\%$  and  $63.4 \pm 6.8\%$ ) when compared to vehicle-treated control cells (Figure 2C). Upon examination of gap junction proteins in monoculture astrocyte cells, NAC treatment for 24hrs induced a significant increase in both connexin-43 ( $60.6 \pm 18\%$ ) and connexin-37 ( $47 \pm 2.8\%$ ) that was not noted after 48hrs of treatment (Figure 2(C&D)).

### 0.0125% NAC is not cytotoxic to endothelial cells or astrocytes in vitro

Although NAC is an FDA-approved drug with few known side effects, slight changes in cell-cell contact could result in BBB permeability differences within this *in vitro* model system. To examine whether NAC has cytotoxic or detrimental effect on the cell morphology, we tested 0.0125% NAC toxicity on cell viability, growth and morphology. 24hrs or 48hrs of NAC treatment did not cause changes in endothelial or astrocyte cell growth or viability (Supplementary Figure 1B & Figure 1D), respectively.<sup>31</sup> In addition, the overall morphology of NAC-treated cells was also similar to controls (Supplementary Figure 1A & Figure C).

than vehicle-treated endothelial cells (data not shown). Data presented in (Figure 4) have been normalized to their respective vehicle-treated control values. NAC treatment for either 24hrs or 48hrs significantly decreased CM-H<sub>2</sub>DCFDA in both cell lines (Figure 3A & Figure 3B).

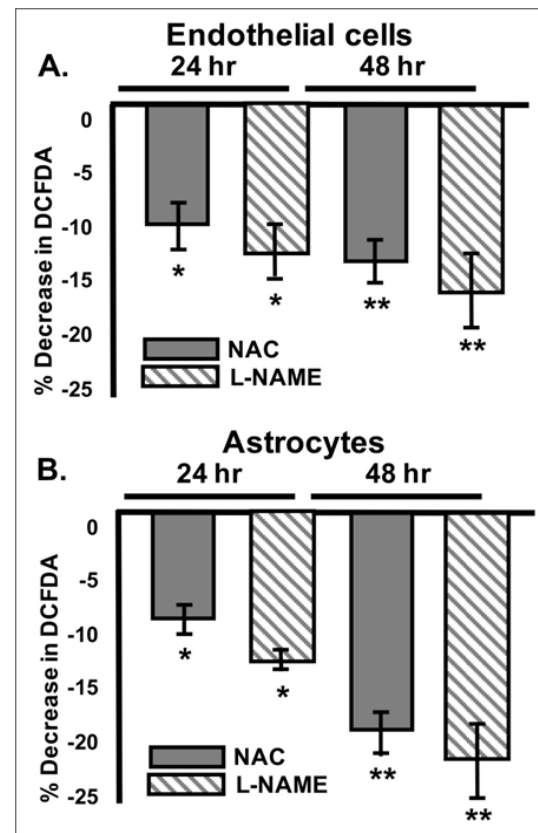
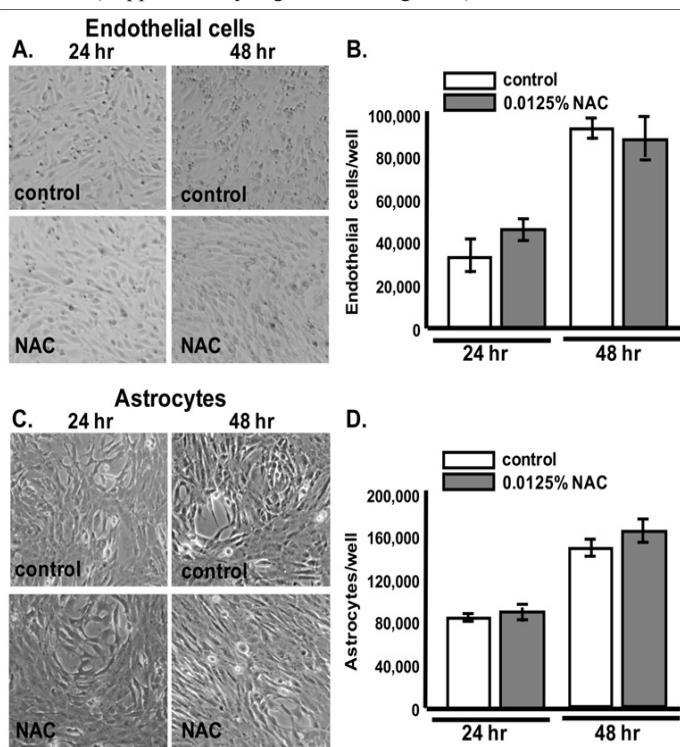


**Figure 3** NAC and L-NAME significantly downregulate reactive oxygen species (ROS). Mean Percent CM-H<sub>2</sub>DCFDA decrease in b End 3 endothelial cells (A) and C8-DIA Astrocytes (B) after administration of 0.0125% NAC (grey) or the NOS inhibitor L-NAME (grey stripe) when compared to vehicle controls. ANOVA with Tukey posthoc analysis. n=3- 6/experiment repeated 3 times. Values represent mean  $\pm$ SD. \* $P < 0.05$ , \*\* $P < 0.01$ .

Our previous work suggests that the nitric oxide synthases (NOSs) may play a specific role in tight and gap junction regulation resulting in BBB permeability changes.<sup>32</sup> CM-H<sub>2</sub>DCFDA is non-specific and detects all ROS levels; therefore, we treated both cell lines with  $\omega$ -Nitro-L-arginine methyl ester hydrochloride (L-NAME), a specific NOS inhibitor that requires hydrolysis of the methyl ester by cellular esterases to become a fully functional inhibitor (L-NNA). However, it is noted that L-NAME also inhibits cGMP formation in endothelial cells. L-NAME was administered to both cell types in order to determine whether NOS may play a role in the NAC-induced ROS downregulation. L-NAME administration for either 24hrs or 48hrs resulted a similar significant decrease in CM-H<sub>2</sub>DCFDA fluorescence to that noted after 0.0125% NAC-treatment alone in both endothelial cells and astrocytes (Figure 3A & Figure 3B) respectively. Similarly, after L-NAME administration, astrocyte ROS levels were reduced  $12.2 \pm 0.81\%$  after 24hrs and  $12.8 \pm 2.0\%$  after 48hrs.

### NAC-induced iNOS and nNOS regulation

There are three major isoforms of nitric oxide synthases that can regulate endothelial and astrocyte junctions; endothelial (eNOS),



**Supplementary (Figure 1A–Figure 1D)** 24hrs or 48hrs of NAC treatment did not cause changes in endothelial or astrocyte cell growth or viability.

### NAC and L-NAME significantly downregulate reactive oxygen species (ROS)

One mechanism by which NAC is thought to regulate multiple pathways is through its antioxidant properties. In order to determine whether the antioxidant properties of NAC- treatment could have played a role in its effects upon BBB permeability, we measured total reactive oxygen species (ROS) in both cell lines using the non-specific ROS indicator CM- H<sub>2</sub>DCFDA in NAC-treated cells compared to vehicle-treated cells. It is interesting to note that vehicle-treated astrocytes produced significantly more reactive oxygen species (ROS)

inducible (iNOS) and neuronal (nNOS). These enzymes convert arginine into citrulline, producing NO in the process. Therefore, the level of NO can be measured using NO synthases activity or expression levels. NOSs can be produced from endothelial cells, astrocytes, microglia, oligodendrocytes, and neurons in the brain. However, whether NAC can affect tight and gap junctions through endothelial and/or astrocytic NOS-dependent mechanism, and which isoform(s) plays a direct role in modulating the BBB permeability is still unclear.<sup>33</sup> To determine which NOS isoforms are modulated specifically in astrocytes or endothelial cells after NAC administration, we treated monocultures of brain endothelial and astrocytes with 0.0125% NAC for 24hrs and 48hrs. Western Blot analysis showed no significant changes in eNOS or iNOS after 24hrs of NAC treatment in the endothelial cells; however, there was a significant 5 fold increase in nNOS at this time (Figure 4A & Figure B).

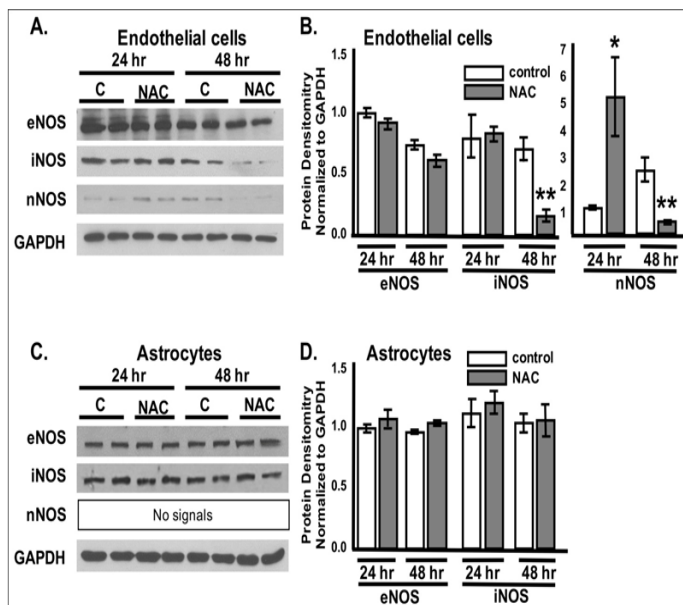


**Figure 4** NAC modulates NOS expression in endothelial cells but not astrocytes. Representative Western blots of bEnd3 endothelial cell (A) and C8-DIA astrocyte (C) lysates from control, vehicle-treated cells labeled “C” and cells post 24hrs or 48hrs NAC treatment labeled “NAC” showing protein expression levels of NOSs (eNOS, iNOS, and nNOS) and the loading control GAPDH. Quantification of protein expression (B, D). ANOVA with Tukey posthoc analysis.  $n = 3-6$ /experiment repeated 3 times. Values represent mean  $\pm$ SD. \* $P < 0.05$ , \*\* $P < 0.01$ .

Interestingly, 48hrs of NAC treatment to endothelial cells resulted in a significant decrease in both iNOS ( $78.8 \pm 3.6\%$ ) and nNOS ( $89.9 \pm 12.9\%$ ) expression levels (Figure 4A & Figure 4B). Alternatively, no changes in NOS expression were noted in the astrocytes at either timepoint (Figure 4C & Figure 4D).

#### 48hrs of NAC treatment alters endothelial cell respiration

The bulk of what is conventionally considered the BBB is made up of brain vascular endothelial cells. These endothelial cells differ from endothelium elsewhere in that they have stronger tight junctions, and are more metabolically active with higher percentages of mitochondria.<sup>34</sup> Mitochondria can produce energy via mitochondrial respiration, and it has long been thought that brain endothelial cells of the BBB require more energy in order to maintain their barrier function.

To investigate the impact of NAC administration on endothelial cell mitochondrial respiration, oxygen consumption was measured via Extracellular Flux Analysis. A model of mitochondrial respiration measurements from this analysis can be found in (Figure 5A). No significant changes in mitochondrial respiration were noted after 24hrs of NAC treatment; (Figure 5B) however, after 48hrs mitochondrial maximal respiration significantly dropped when compared to vehicle-treated controls (Figure 5C & Figure 5D). Maximal respiration can be calculated using oxygen consumption after the electron transport chain was uncoupled from oxidative phosphorylation using FCCP. Because oxygen consumption in cells can be non-mitochondrial, respiration specific to the cellular non-mitochondrial component can be assessed by inhibiting mitochondrial Complex I and Complex III with rotenone and Antimycin A. 48 hours of NAC treatment also significantly reduced the non-mitochondrial oxygen consumption rate (OCR) (Figure 5E);  $p < 0.0004$ .

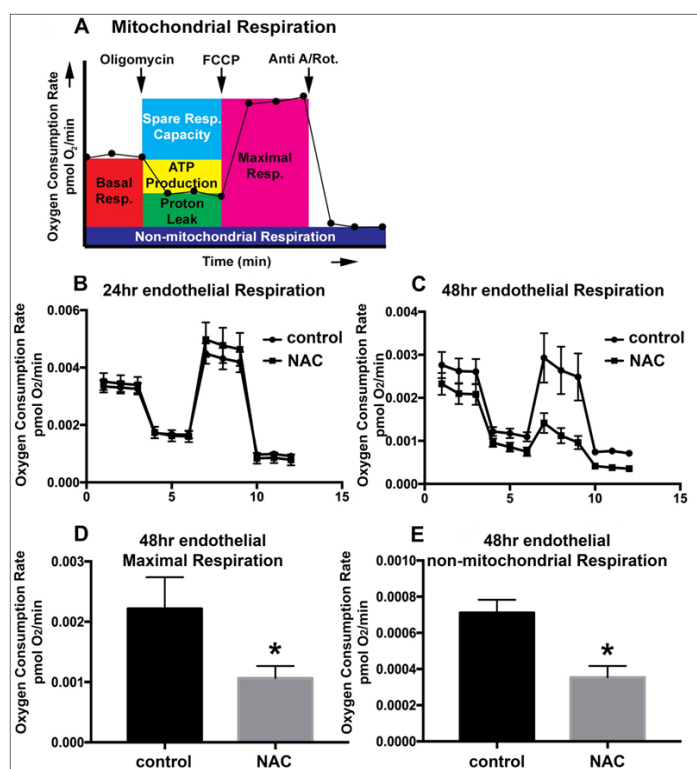


**Figure 5** 48hrs of NAC treatment alters endothelial cell respiration. Model of Extracellular Flux Analysis utilizing the Mitochondrial Stress Test (A). Extracellular Flux Analysis for vehicle-treated control bEnd3 endothelial cells (circle) and those treated with 0.125% NAC (square) for 24hrs (B) or 48hrs (C). Oxygen consumption rates are expressed as mean  $\pm$  SEM and are normalized to the number of cells seeded, denoted fmol O<sub>2</sub>/min/cell (y-axis). The x-axis represents time in minutes. Quantification of maximal respiration (D) and non-mitochondrial respiration (E) for endothelial cells after 48hours of NAC treatment. Two-way ANOVA with Tukey's multiple comparisons test.  $n = 5-10$ /experiment repeated 3 times. Values represent mean  $\pm$ SD. \* $P < 0.05$ .

#### NAC-induced endothelial mitochondrial connexin-43 and complex i alterations are time-dependent

While it is commonly known that connexin-43 is found at the plasma membrane and within the nucleus where it can signal and/or form gap junctions, our lab and others have recently found the presence of connexin-43 in the mitochondrial membrane. It has been suggested that mitochondrial connexin<sup>35</sup> can interact with electron chain transport proteins and reduce ROS formation after



preconditioning stimuli<sup>29</sup>. To determine whether mitochondrial-specific connexin<sup>36</sup> and electron chain transport proteins are altered after NAC administration in endothelial cells, mitochondrial proteins were extracted using high speed ultracentrifugation and examined via Western Blot analysis. Although no significant differences were noted after 24hrs of NAC treatment in the Extracellular Flux experiments, NAC-induced a significant increase in connexin-43 and Complex I after 24hrs (Figure 6A & Figure 6C). However, the significant decrease in Maximal respiration noted after 48hrs of NAC treatment (Figure 5) was mirrored by significant reductions in connexin-43, Cytochrome C, Complex I, and UCP-2 protein expression (Figure 6A & Figure 6C), Figure 6E & Figure 6F). No significant changes were noted after 24 or 48hrs of NAC treatment for the electron transport chain protein Complex V (Figure 6A & Figure 6D).

Astrocytic endfeet surround endothelial vasculature and promote the tightness of endothelial tight junctions<sup>12</sup>. These endfeet transport a variety of components in and out of the brain through an assortment of mechanisms including gap junctions. In disease situations, mitochondria have been shown to accumulate in swollen astrocytic endfeet, indicating that they are very metabolically active and may respond to ROS accumulation<sup>17</sup>. To investigate the impact of NAC administration on astrocyte mitochondrial respiration, oxygen consumption was measured via Extracellular Flux Analysis. A model for mitochondrial respiration quantification is shown in (Figure 7A). Resting oxygen consumption (i.e. basal respiration) was significantly increased after 24hrs of NAC treatment (Figure 7B & Figure 7C). To test the maximal respiration rate that astrocytes could achieve, the electron transport chain was uncoupled from oxidative phosphorylation using FCCP. 24hrs of NAC treatment also significantly increased the cells maximal respiration (Figure 7D).

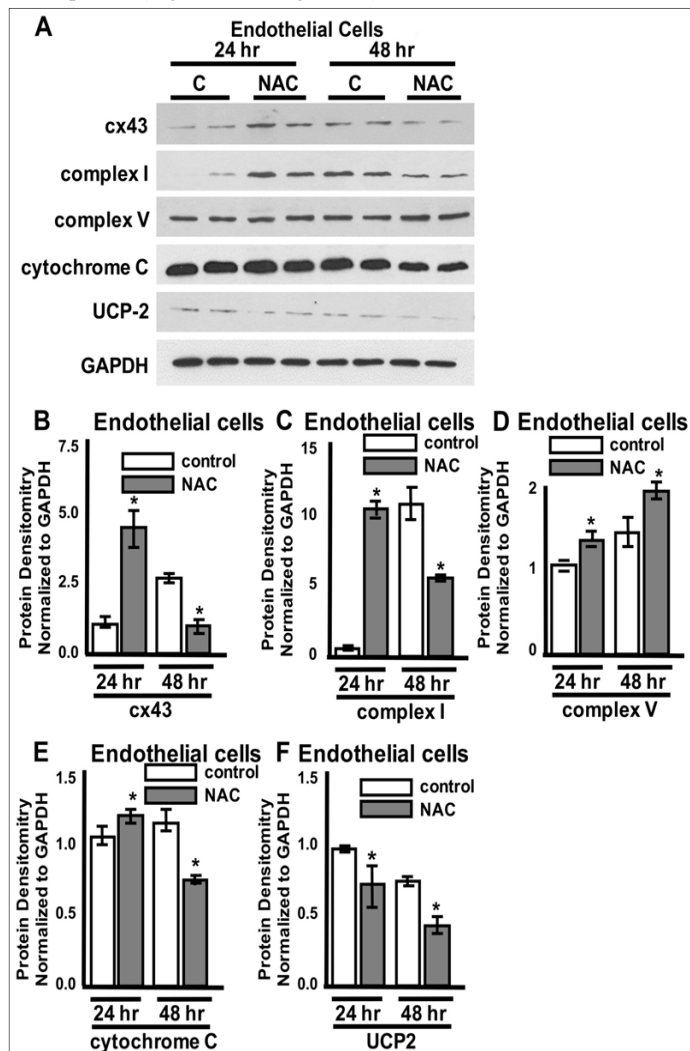


**Figure 6** NAC-induced endothelial mitochondrial connexin-43 and complex i alterations are time-dependent. Representative Western blots from protein lysates isolated from the mitochondria of bEnd3 endothelial cells from control, vehicle-treated cells labeled "C" and cells post NAC treatment for 24hrs or 48hrs labeled "NAC". Quantification of protein expression for connexin- 43 (cx43) (B), complex I (C), complex V (D), cytochrome C (E), and UCP2 (F). GAPDH was used as a loading control. ANOVA with Tukey's multiple comparisons test. n=3-5/ experiment repeated 3 times. Values represent mean  $\pm$  SD. \*P<0.05.

### NAC-induced metabolic changes in astrocytes are time-dependent

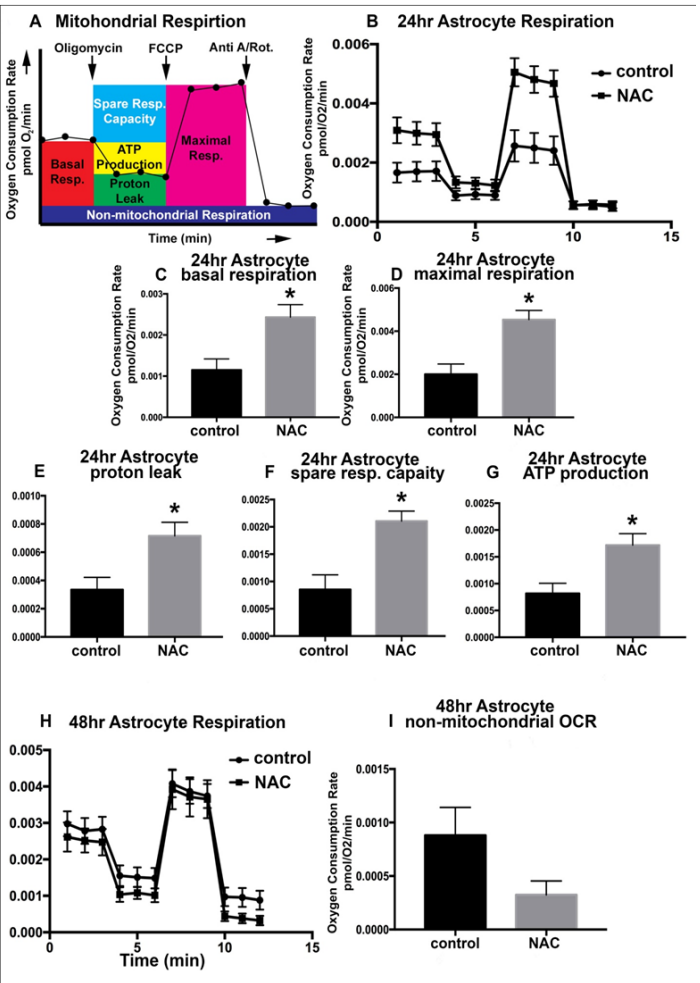


**Figure 7** NAC-induced metabolic changes in astrocytes are time-dependent. Model of Extracellular Flux Analysis utilizing the Mitochondrial Stress Test (A). Extracellular Flux Analysis for vehicle-treated control C8-D1A astrocytes (circle) and those treated with 0.125% NAC (square) for 24hrs (B) or 48hrs (H). Oxygen consumption rates are expressed as mean  $\pm$  SEM and are normalized to the number of cells seeded, denoted fmol O<sub>2</sub>/min/cell (y-axis). The x-axis represents time in minutes. Quantification of basal respiration (C) and maximal respiration (D), proton leak (E), spare respiratory capacity (F), and ATP production (G) after 24 hours of NAC treatment in C8-D1A astrocytes. Quantification of the non-mitochondrial oxygen consumption rate (OCR) after 48 hours of 0.125% NAC treatment (I). ANOVA with Tukey's multiple comparisons test. n=5-10/experiment repeated 3 times. Values represent mean  $\pm$  SD. \*P<0.05.

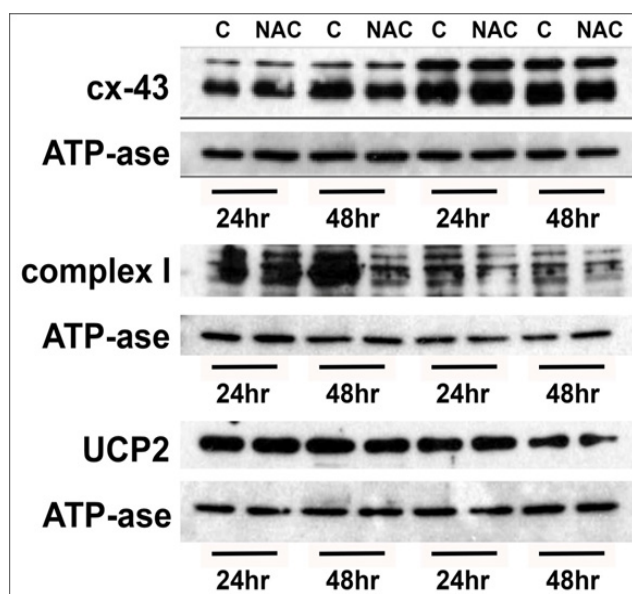
Oxygen is consumed to establish a proton gradient across the inner mitochondrial membrane. This gradient supports both ATP production and proton leak. The fraction of basal respiration associated with ATP production is referred to as coupling efficiency. 24hrs of NAC administration results in a significant increase ( $p < 0.0056$ ) in astrocyte coupling efficiency (Figure 7G). Coupling efficiency is impacted by the amount of proton leak from the inner membrane space back into the mitochondrial matrix. NAC treatment for 24hrs also induced a significant increase ( $p < 0.008$ ) in astrocyte proton leak (Figure 7E). Basal respiration includes proton leak; therefore, quantitation of proton leak is typically reported as a fraction of proton leak/basal respiration.

We also calculated the capability of the cells to respond to increased energy demands, termed the spare respiratory capacity. This parameter also describes how close basal respiration is to the maximal respiratory rate. Therefore, with both basal and maximal respiration increased, it is of no surprise that there was a significant increase in the Astrocyte spare respiratory capacity after 24hrs of NAC treatment (Figure 7F).

With significant changes in several aspects of mitochondrial respiration and output after 24hrs of NAC treatment, it was surprising that 48hrs of treatment did not result in significant changes when compared to vehicle-treated controls (Figure 7H). The one parameter that did decrease in a non-significant trend after 48hrs of NAC treatment was the amount of non- mitochondrial OCR (Figure 7I),  $p < 0.07$ .

#### NAC treatment does not alter astrocyte mitochondrial proteins

No significant changes were noted in the astrocytic mitochondrial fraction concentrations of connexin-43, complex I, or UCP2 after 24 hours or 48 hours of NAC exposure (Supplementary Figure 2)

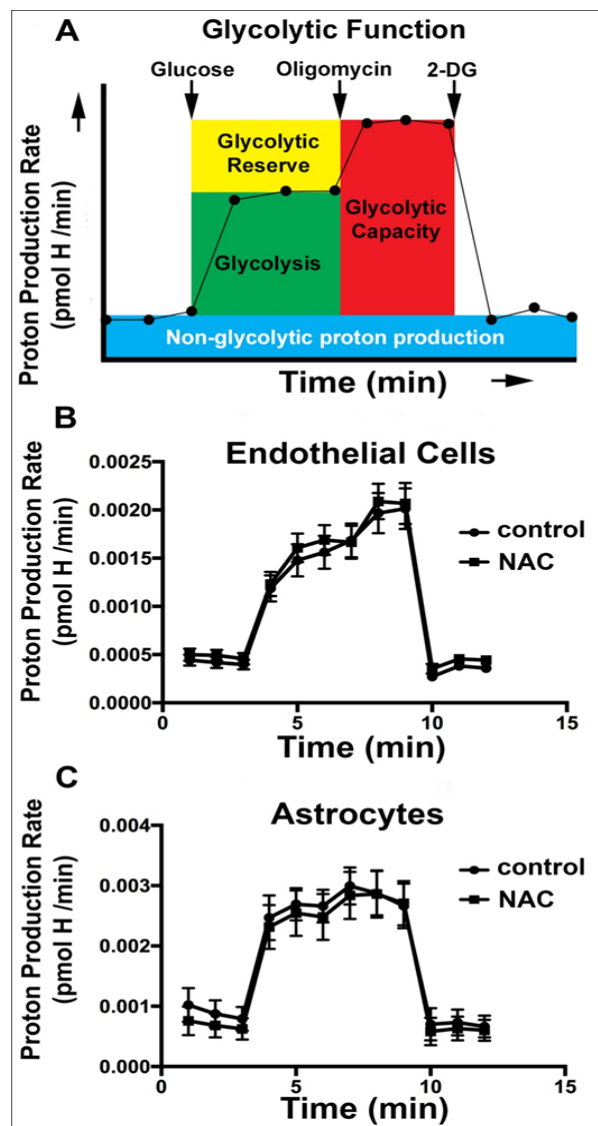


**Supplementary Figure 2** UCP2 after 24 hours or 48 hours of NAC exposure.

#### NAC treatment does not alter endothelial or astrocyte glycolysis

Cells can produce energy through glycolysis or mitochondrial respiration. To determine whether NAC can alter glycolysis, we

measured oxygen consumption and extracellular pH via Extracellular Flux Analysis to investigate the extracellular acidification rate (ECAR) of endothelial cells or astrocytes with or without NAC treatment. NAC did not alter the Basal or resting glycolysis in either cell type (Supplementary Figure 3). In addition, no significant differences were found in the glycolytic capacity, defined as the highest rate of glycolysis the cells can achieve after ATP synthase is inhibited using oligomycin.



**Supplementary Figure 3** NAC did not alter the basal or resting glycolysis in either cell type.

#### Discussion

Delivery of an effective drug to the Central Nervous System (CNS) through the BBB is a therapeutic issue that has not been effectively addressed. The BBB excludes more than 98% of all small-molecule drugs and almost 100% of large-molecule therapeutics, such as peptides, proteins, antibodies, RNA interference (RNAi)-based drugs and gene vectors.<sup>30</sup> Several drugs of potential therapeutic value do not readily enter the brain because they have low lipid solubility and are not transported by specific carriers. To overcome this limitation, researchers around the globe have investigated several strategies such as intrathecal injection, direct *in vivo* gene therapy (intracranial



or systemic vector delivery), small molecule therapies (substrate reduction and chaperone therapy) and cell-based therapies.<sup>37-40</sup> Others have also focused on increasing the permeability of the BBB by changing BBB osmolality, treating with vasoactive compounds such as Bradykinin and its analog RPM-7 (B2 receptor agonist), and targeting inflammatory response components, such as small Ras-related GTPases, Rho, Rho kinase, and PKC isoforms. However, a transient “opening” of BBB, in normal and pathological conditions, and the side effect of therapies currently used to open this barrier are still under investigation. Thus, finding an agent(s) that can act as an “on-and off-switch” for the BBB will potentially enable clinicians to control efficient transfer of drugs to the brain and prevent or treat the adverse effects of BBB disruption in disease conditions. This is a complex issue, and few studies have examined the plasticity of BBB permeability over time.

The antioxidant N-acetylcysteine (NAC) has proven to be beneficial in multiple animal and clinical trials for a variety of neuropsychiatric and neurodegenerative diseases that are thought to involve BBB permeability issues including epilepsy, Alzheimer’s and Parkinson’s disease, ALS, stroke, encephalitis, multiple sclerosis, depression, schizophrenia, and bipolar disease;<sup>19</sup> however, its mechanism of action on the brain vascular endothelial cells and astrocytes that make up the BBB have not been elucidated. Because metabolic respiration, and it’s cellular biproduct reactive oxygen species (ROS), has been linked to the regulation of BBB tight and gap junctions, this study aimed to determine whether NAC-induced BBB permeability changes do indeed correlate with both functional metabolic alterations and tight and gap junction changes.

Our previous studies have shown that NAC can alter blood-brain barrier (BBB) permeability in mice via changes in ROS. This study showed BBB permeability modulation in a time and dose-dependent fashion using NAC administration in an *in vitro* mouse BBB model system consisting of brain microvascular endothelial and cerebrum astrocytic cells. The present study shows that the response of a murine *in-vitro* BBB model to NAC treatment is time- dependent, becoming leakier in the first 24 hours and tighter after 48 hours of exposure. Our data fit with the hypothesis that the BBB permeability is in a constant state of flux with the cells responding to their environment. Therefore, understanding what causes alterations in permeability in one direction or the other may allow us to utilize this natural biology to aide in drug delivery to the brain.

Permeability changes correlated with NAC-induced reduction in endothelial tight junction proteins, mainly occludin, and increased astrocytic gap junctions connexin-37 and -43 after 24 hours. Continuous treatment of cells with NAC for 48hrs reduced tight junction levels further in endothelial cells, restored gap junctions in astrocytes, and decreased BBB permeability. Although NAC treatment for 24hrs did not have any significant effect on claudin-5 expression, immune histochemistry revealed an alteration in its localization within the cell.

Claudin-5 cellular dispersion in combination with the decrease in occludin expression levels may have been sufficient to disrupt BBB integrity in this model. Our result also indicates that NAC effects both endothelial and astrocytic cells. These cell types usually work side by side to maintain the integrity of BBB, and have been hypothesized to be capable of influencing one another. The reduction in tight junction expression levels was combined with an increase in gap junction proteins in astrocytes, possibly providing credence to this theory. The importance of astrocytes and gap junctions in BBB function has been indicated in a recent study showing that disruption of BBB integrity

can occur by a GJ-dependent mechanism;<sup>13</sup> however, how astrocytic GJs modulate BBB permeability is not known. Unexpectedly, even though connexin-43 (and gap junctions in general) have not been as widely associated with BBB permeability as their tight junction counterparts, connexin-43 expression levels mimicked permeability much better than the tight junctions commonly associated with BBB tightness (claudin-5 and occludin). In this study, 24hrs of NAC induced an increase in connexin-43 expression that correlated to an increase in BBB permeability in both endothelial cells and astrocytes. However, 48hrs of NAC treatment resulted in reduced connexin-43 expression and decreased permeability.<sup>12</sup> Possible novel role of connexins found both in brain vascular endothelial cells and astrocytes in BBB permeability modulation. Their conclusions suggest that plasma membrane proteins that handle calcium, tight junction proteins, and connexins combine into a macrocomplex that can influence endothelial permeability; however, studies elucidating the extensive role of connexins in BBB permeability are just now coming to light.

Metabolic respiration within brain capillary endothelial cells are also important to BBB function. Highly active endothelial cells at the blood-brain barrier have a higher mitochondrial content (8–11%) compared to endothelial cells in other capillary beds.<sup>28</sup> This increase in mitochondria has led to the assumption that brain vascular endothelial cells require more energy to perform their barrier functions. It is known that cellular ATP plays a role in regulating the brain endothelial tight junctions and BBB permeability.<sup>41-45</sup> Therefore, mitochondria play a vital role in BBB permeability alongside cellular tight and gap junctions. While mitochondrial dysfunction is also a co-founding symptom found in both BBB disruption and most neurodegenerative diseases<sup>15-16</sup>, the concept that the mitochondrial dysfunction causes the BBB permeability issues is novel.

In this study we examined the role of NAC-induced BBB changes on mitochondrial function. NAC is known to upregulate both glutathione and mitochondrial complex I, and can rescue the oxidative stress in preclinical models of mitochondrial complex I disease. Both of these proteins perform the redox function of reducing NADPH to NADP<sup>+</sup> + H<sup>+</sup>; therefore, these are two pathways that may explain a portion of NAC’s antioxidant function within cells.

Knockdown of mitochondrial connexin-43 results in a decrease in Complex I and concomitant decreased mitochondrial respiration, while overexpression results in the opposite (increased complex I and mitochondrial respiration).<sup>43</sup> Our data show a parallel finding. NAC-induced upregulation of mitochondrial connexin-43, upregulation of Complex I, decreased ROS, and increased respiration after 24hours of treatment that correlate to leakier BBB permeability.

Alternatively, after 48hrs of NAC treatment, mitochondrial connexin-42 and Complex I were reduced, respiration went back to normal levels, and BBB permeability significantly tightened. The well-established correlation between mitochondrial connexin-42 and Complex I expression leads us to suggest that NAC may regulate mitochondrial Complex I through its regulation of mitochondrial connexin-42. Future studies are needed to determine this possible relationship.

Although NAC is known to specifically regulate NADPH through glutathione and Complex I, its antioxidant properties have not been cited to be specific. Therefore, general examination of total ROS levels was necessary in order to begin to understand a portion of NAC’s redox function(s). Nitric oxide (NO) is one mediator that regulates vascular permeability in complex ways. Low NO levels help maintain

of endothelial integrity<sup>44</sup>, and high NO concentrations induce BBB breakdown. As reviewed by,<sup>31</sup> many of the inductive effects on brain endothelium are produced by astrocytes including NO. We also have shown that NO produced from oligodendrocytes modulates TJ and GJ proteins in surrounding astrocytes and endothelial cells in a non-cell autonomous fashion, affecting brain permeability and contributing to behavioral abnormalities *in vivo*. Upon examining NOS isoforms, only endothelial cell nNOS reflected changes in BBB permeability in this system, with increased expression correlating to increased BBB permeability and decreased expression found when BBB permeability decreased. Our data are consistent with reports that suggest an interdependent function between NOSs/NO signaling and TJ and GJ communication<sup>46-48</sup>. Furthermore, our metabolic data link nNOS, connexin-43, and mitochondrial Complex I expression to mitochondrial respiration and BBB permeability status. This data support previous findings in cardiomyocytes after ischemia that show conditional overexpression of nNOS causes its translocation to the mitochondria, inhibited mitochondrial function, and reduced ROS generation.<sup>46-48</sup>

Interestingly, while NAC did induce a decrease in total ROS expression, no changes in NOS expression were noted in the astrocytes at either time-point. One explanation for this can be noted in the significant reduction of non-mitochondrial OCR after 48hrs of NAC treatment. This data suggests that the reduction in redox noted in astrocytes is probably occurring outside of the mitochondria. Together, our data indicate that NAC has a significant effect on NOSs expression level modulation, specifically in endothelial cells, and particularly on the nNOS isoform. Changes in nNOS were accompanied by changes in BBB permeability and TJ expression. The reasons each NOS isoform responded differently to the NAC treatment are not entirely clear. However, it is important to note that both iNOS and nNOS are soluble proteins whereas eNOS is a membrane bound protein. In addition, in resting cells both eNOS and nNOS are constitutively expressed while iNOS is an inducible protein that is more active in response to an insult or injury of the cell.

NAC-induced mitochondrial complex I, cytochrome C, and UCP-2 expression levels were down regulated in endothelial cells indicating that NAC alters mitochondrial function. This was further supported by extracellular flux analysis that revealed NAC-induced a significant reduction in mitochondrial maximal respiration. Surprisingly, this mitochondrial effect of NAC was endothelial cell specific after 48 hours of NAC treatment. In contrast, astrocyte metabolism (in terms of basal and maximal respiration, and ATP coupling efficiency) was significantly up regulated after 24 hours of NAC treatment, and showed no change after 48 hours. These changes correspond to alterations in ROS (specifically NOS) in endothelial cells but not in astrocytes. Our results indicate that NAC modulates mitochondrial respiration in conjunction with BBB permeability differentially in astrocytes and endothelial cells.

Our previous studies have shown that NAC can alter blood-brain barrier (BBB) permeability in mice via changes in ROS. This study showed BBB permeability modulation in a time and dose-dependent fashion using NAC administration in an *in vitro* mouse BBB model system consisting of brain microvascular endothelial and cerebrum astrocytic cells. The present study shows that the response of a murine *in-vitro* BBB model to NAC treatment is time-

dependent, becoming leakier in the first 24 hours and tighter after 48 hours of exposure. Our data fit with the hypothesis that the BBB permeability is in a constant state of flux with the cells responding to their environment. Therefore, understanding what causes alterations

in permeability in one direction or the other may allow us to utilize this natural biology to aide in drug delivery to the brain.

## Author contributions

SSE, CAW, LH, CS performed experiments and aided in data analysis and figure development. DAM conceived of experiments, analyzed data, and wrote and edited the manuscript.

## Acknowledgements

This work was supported in part by funding from a Wright State University Research Initiation Grant and Wright State University start-up funding to DAM.

## Conflict of interest

The authors declare that they have no conflicts of interest with the contents of this article.

## References

1. Persidsky Y, Ramirez SH, Haorah J, et al. Blood-brain barrier: Structural components and function under physiologic and pathologic conditions. *J Neuroimmune Pharmacol*. 2006;1(3):223–236.
2. Zlokovic BV. The blood-brain barrier in health and chronic neurodegenerative disorders. *Neuron*. 2008;57(2):178–201.
3. Huber JD, Eggleston RD, Davis TP. Molecular physiology and pathophysiology of tight junctions in the blood-brain barrier. *Trends Neurosci*. 2001;24(12):719–725.
4. Nitta T, Hata M, Gotoh S, et al. Size selective loosening of the blood-brain barrier in claudin-5-deficient mice. *J Cell Biol*. 2003; 161(3):653–660.
5. Hirase T, Staddon JM, Saitou M. Occludin as a possible determinant of tight junction permeability in endothelial cells. *J Cell Sci*. 1997;110(pt 14):1603–1613.
6. Bolton SJ, Anthony DC, Perry VH. Loss of the tight junction proteins occludin and zonula occludens-1 from cerebral vascular endothelium during neutrophil-induced blood-brain barrier breakdown *in vivo*. *Neuroscience*. 1998;86(4):1245–1257.
7. Dallasta LM, Pizarov LA, Esplen JE, et al. Blood-brain barrier tight junction disruption in human immunodeficiency virus-1 encephalitis. *Am J Pathol*. 1999;155(6):1915–1927.
8. Tang Z, Guo D, Xiong L, et al. TLR4/PKCα/occluding signaling pathway may be related to blood-brain barrier damage. *Mol Med Rep*. 2018;18(1):1051–1057.
9. Wu L, Ye Z, Pan Y, et al. Vascular endothelial growth factor aggravates cerebral ischemia and reperfusion-induced blood-brain-barrier disruption through regulating IκB102640519/HOXC13/ZO-1 signaling. *Exp Cell Res*. 2018;369(2):275–283.
10. Rakkar K, Bayraktutan U. Increases in intracellular calcium perturb blood-brain barrier via protein kinase C-α and apoptosis. *Biochimica et Biophysica Acta*. 2016.1862(1):56–71.
11. De Bock M, Wang N, Decrock E, et al. Endothelial calcium dynamics, connexin channels and blood-brain barrier function. *Prog Neurobiol*. 2013;108:1–20.
12. Eugenini EA, Clements JE, Zink MC, et al. Human immunodeficiency virus infection of human astrocytes disrupts blood-brain barrier integrity by a gap junction-dependent mechanism. *J Neurosci*. 2011;31(26):9456–9465.
13. Palmer AM. The role of the blood brain barrier in neurodegenerative disorders and their treatment. *J Alzheimers Dis*. 2011;24(4):643–656.
14. Yao J & Brinton RD. Estrogen Regulation of Mitochondrial Bioenergetics:

- Implications for Prevention of Alzheimer's Disease. *Adv Pharmacol.* 2012;64:327–371.
15. Johri A, Beal MF. Mitochondrial Dysfunction in Neurodegenerative Diseases. *J Pharmacol Exp Ther.* 2012;342(3):619–630.
16. Mayes DA, Rizvi TA, Titus Mitchell H, et al. Nfl loss and Ras hyperactivation in oligodendrocytes induce NOS-driven defects in myelin and vasculature. *Cell Rep.* 2013;4(6):1197–1212.
17. Berk M, Malhi GS, Gray LJ, et al. The promise of N-acetylcysteine in Neuropsychiatry. *Trends Pharmacol Sci.* 2013;34(3):167–77.
18. Daneman R. The Blood-Brain Barrier in Health and Disease. *Ann Neurol.* 2012;72(5):648–672.
19. Brown RC, Morris AP, O Neil RG. Tight junction protein expression and barrier properties of immortalized mouse brain microvessel endothelial cells. *Brain Res.* 2007;1130(1):17–30.
20. Chen F, Hori T, Ohashi N, et al. Occludin is regulated by epidermal growth factor receptor activation in brain endothelial cells and brains of mice with acute liver failure. *Hepatology.* 2011; 53(4):1294–1305.
21. Kapitulnik J, Benaïm C, Sasson S. Endothelial Cells Derived from the Blood-Brain Barrier and Islets of Langerhans Differ in their Response to the Effects of Bilirubin on Oxidative Stress Under Hyperglycemic Conditions. *Front Pharmacol.* 2012;3:131.
22. Oldendorf WH, Cornford ME, Brown WJ. The large apparent work capability of the blood-brain barrier: a study of the mitochondrial content of capillary endothelial cells in brain and other tissues of the rat. *Ann Neurol.* 1977;1(5):409–417.
23. Fleegal MA, Hom S, Borg LK, et al. Activation of PKC modulates blood-brain barrier endothelial cell permeability changes induced by hypoxia and posthypoxic reoxygenation. *Am J Physiol Heart Circ Physiol.* 2005;289(5):2012–2019.
24. Peng J, He F, Zhang C, et al. Protein kinase C- $\alpha$  signals P115RhoGEF phosphorylation and RhoA activation in TNF- $\alpha$ -induced mouse brain microvascular endothelial cell barrier dysfunction. *J Neuroinflammation.* 2011;8:28.
25. Predescu D, Predescu S, Shimizu J, et al. Constitutive eNOS-derived nitric oxide is a determinant of endothelial junctional integrity. *Am J Physiol Lung Cell Mol Physiol.* 2005;289(3):371–381.
26. Willis CL, Meske DS, Davis TP. Protein kinase C activation modulates reversible increase in cortical blood-brain barrier permeability and tight junction protein expression during hypoxia and posthypoxic reoxygenation. *J Cereb Blood Flow Metab.* 2010;30(11):1847–1859.
27. Mandel LJ, Bacallao R, Zampighi G. Uncoupling of the molecular “fence” and paracellular “gate” functions in epithelial tight junctions. *Nature.* 1993;361(6412):552–555.
28. Canfield PE, Geerdes AM, Molitoris BA. Effect of reversible ATP depletion on tight-junction integrity in LLC-PK1 cells. *Am J Physiol.* 1991;261(6 pt2):1038–1045.
29. Ye J, Tsukamoto T, Sun A, et al. A role for intracellular calcium in tight junction reassembly after ATP depletion-repletion. *Am J Physiol.* 1999;277(4):524–532.
30. Oppenheim HA, Lucero J, Guyot AC, et al. Exposure to vehicle emissions results in altered blood brain barrier permeability and expression of matrix metalloproteinases and tight junction proteins in mice. *Part Fibre Toxicol.* 2013;10:62.
31. Haseloff RF, Blasig IE, Bauer HC, et al. In search of the astrocytic factor(s) modulating blood-brain barrier functions in brain capillary endothelial cells *in vitro*. *Cell Mol Neurobiol.* 2005;25(1):25–39.
32. Liu J, Jin X, Liu KJ, et al. Matrix metalloproteinase-2-mediated occludin degradation and caveolin-1-mediated claudin-5 redistribution contribute to blood-brain barrier damage in early ischemic stroke stage. *J Neurosci.* 2012;32(9):3044–3057.
33. Kurihara T, Westenskow PD, Krohne TU, et al. Astrocyte pVHL and HIF- $\alpha$  isoforms are required for embryonic-to-adult vascular transition in the eye. *J Cell Biol.* 2011;195:689–701.
34. Boengler K, Ruiz Meana M, Gent S, et al. Mitochondrial connexin 43 impacts on respiratory complex I activity and mitochondrial oxygen consumption. *J Cell Mol Med.* 2012;16(8):1649–1655.
35. Polyak E, Ostrovsky J, Peng M, et al. N-acetylcysteine and vitamin E rescue animal longevity and cellular oxidative stress in pre-clinical models of mitochondrial complex I disease. *Mol Genet Metab.* 2018;123(4):449–462.
36. Boengler KA, Ruiz Meana MB, Gent SA, et al. Mitochondrial connexin 43 impacts on respiratory complex I activity and mitochondrial oxygen consumption. *J Cell Mol Med.* 2012;16(8):1649–1655.
37. Booth R, Kim H. Characterization of a microfluidic *in vitro* model of the blood-brain barrier ( $\mu$ BBB). *Lab Chip.* 2012;12(10):1784–1792.
38. Sharif Y, Jumah F, Coplan L, et al. The Blood Brain Barrier: A Review of its Anatomy and Physiology in Health and Disease. *Clin Anat.* 2018.
39. Bartus RT, Elliott P, Hayward N, et al. Permeability of the blood brain barrier by the bradykinin agonist, RMP-7: evidence for a sensitive, auto-regulated, receptor-mediated system. *Immunopharmacology.* 1996;33(1–3):270–278.
40. Laterra J, Keep R, Betz LA, et al. Blood-Brain Barrier. In: Siegel GJ, Agranoff BW, et al, editors. *Basic Neurochemistry: Molecular, Cellular and Medical Aspects.* 1999.
41. Ellis SL, Gysbers V, Manders PM, et al. The cell-specific induction of CXC chemokine ligand 9 mediated by IFN- $\gamma$  in microglia of the central nervous system is determined by the myeloid transcription factor PU.1. *J Immunol.* 2010;185(3):1864–1877.
42. Lasram MM, Dhouib IB, Annabi A, et al. A review on the possible molecular mechanism of action of N-acetylcysteine against insulin resistance and type-2 diabetes development. *Clin Biochem.* 2015;48(16–17):1200–1208.
43. Garg T, Bhandari S, Rath G, et al. Current strategies for targeted delivery of bio-active drug molecules in the treatment of brain tumor. *J Drug Target.* 2015;23(10):865–887.
44. Prados MD, Schold SC JR SC, Fine HA, et al. A randomized, double-blind, placebo-controlled, phase 2 study of RMP-7 in combination with carboplatin administered intravenously for the treatment of recurrent malignant glioma. *Neuro Oncol.* 2003;5(2):96–103.
45. Spindler V, Schlegel N, Waschke J. Role of GT Pases in control of microvascular permeability. *Cardiovasc Res.* 2010;87(2):243–253.
46. Kameritsch P, Khandoga N, Nagel W, et al. Nitric oxide specifically reduces the permeability of Cx37-containing gap junctions to small molecules. *J Cell Physiol.* 2005;203(1):233–242.
47. Brott DA, Richardson RJ, Loudon CS. Evidence for the nitric oxide pathway as a potential mode of action in fenoldopam-induced vascular injury. *Toxicol Pathol.* 2012;40(6):874–886.
48. Burkard N, Williams T, Czolbe M, et al. Conditional overexpression of neuronal nitric oxide synthase is cardioprotective in ischemia/reperfusion. *Circulation.* 2010;122(16):1588–1603.